7434 *Macromolecules* **2010**, *43*, 7434–7445
DOI: 10.1021/ma101452h

Macromolecules
ARTICLE

Synthesis and Self-Assembly of Amphiphilic Asymmetric Macromolecular Brushes

Xueming Lian, Dongxia Wu, Xiaohui Song, and Hanying Zhao*

Key Laboratory of Functional Polymer Materials, Ministry of Education, Department of Chemistry, Nankai University, Tianjin 300071, P. R. China

Received January 13, 2010; Revised Manuscript Received August 9, 2010

ABSTRACT: Two well-defined amphiphilic asymmetric macromolecular brushes, one bearing hydrophilic poly(ethylene glycol) (PEO) and hydrophobic polystyrene (PS) side chains on poly(glycidyl methacrylate) (PGMA) backbone and the other bearing pendant PEO and poly(styrene-block-*N*-isopropylacrylamide) (PS-*b*-PNIPAM) block copolymer side chains, were synthesized by grafting from approach based on a combination of click chemistry and in situ reversible addition−fragmentation chain transfer (RAFT) polymerization. PGMA backbone was synthesized by atom transfer radical polymerization (ATRP), and a polymer backbone with pendant hydroxyl and azide groups (PGMA−OH/N_3) was obtained after ring-opening reaction of the epoxide rings on PGMA. RAFT chain transfer agent (CTA) was introduced to the polymer backbone by facile click reaction between alkyne-terminated RAFT CTA and PGMA−OH/N_3. PEO side chains were grafted onto the polymer backbone by esterification between carboxyl end group of PEO and hydroxyl group on the polymer backbone; PS or PS-*b*-PNIPAM side chains were prepared by RAFT polymerization. Gel permeation chromatograph, FTIR and ^{1}H NMR results all indicated successful synthesis of well-defined amphiphilic asymmetric macromolecular brushes. The self-assembly of the macromolecular brushes in solutions was also investigated in this research. Asymmetric macromolecular brushes with PEO and PS side chains self-assembled into vesicle structures in methanol. PS side chains were in the walls of the vesicles, and PEO side chains were in the coronae. The average size of the structure increased with PS chain length. The macromolecular brushes with PEO and PS-*b*-PNIPAM block copolymer side chains were able to self-assemble into vesicles in aqueous solution. Temperature exerted a significant effect on the morphology of the structures. At a temperature above lower critical solution temperature (LCST) of PNIPAM, the size of the vesicles decreased due to the shrinking of PNIPAM blocks in the corona.

Introduction

In recent years, polymers with different topological structures, for example, linear block, gradient graft, comb-shaped, star-shaped, hyperbranched, and dendritic copolymers, have been synthesized with the purpose to establish architecture−property relationships and to study self-assembly properties either at solid state or in solution.[1,2] Of all the polymers, macromolecular brushes (also called comb polymers) are attractive polymers because of their unique chemical and physical properties.[3−5] Macromolecular brushes are a type of macromolecules with densely grafted side chains on a linear backbone.[6] Because of the crowded side chains on the backbone, the brush polymers adopt a worm-like cylindrical brush conformation, in which the side chains are stretched in the direction to the backbone.[7]

Macromolecular brushes can be categorized into one-component brushes with homopolymer side chains[8−11] and multicomponent brushes with different pendant side chains.[12−18] For multicomponent macromolecular brushes, there are three different architectures, i.e., double-cylinder type, prototype, and block-type macromolecular brushes.[19,20] Double-cylinder macromolecular brushes are the type of brush polymers with block copolymer side chains on the backbones.[13,21−24] Block-type macromolecular brushes comprise two or more homopolymer brush blocks linked by covalent bonds.[25−27] If there are more than two different side chains on a polymer backbone, this brush polymer is called prototype macromolecular brushes.[12,28,29] The multicomponent copolymer brushes have nanosized phase separation at solid state, even on a brush polymer chain.[20,30] Brush polymers with two different side chains on each repeating unit of the backbone are called asymmetric macromolecular brushes.[31,32] Asymmetric macromolecular brushes have well-defined structures and many interesting properties. For example, amphiphilic asymmetric macromolecular brushes are able to self-assemble into micelles in selective solvents.[31]

Macromolecular brushes can be synthesized through three main approaches, i.e., grafting through (polymerization of macromonomers by a variety of polymerization techniques),[3,33] grafting onto (attachment of polymer chains to the backbone via specific interactions or chemical reactions),[3,34] and grafting from (attachment of initiator molecules to the backbone and growing of polymer chains via in situ polymerization).[3,25,35] In the grafting onto approach, the grafting density is limited due to the steric hindrance. Macromolecular brushes with high grafting density can be prepared by grafting from method. In the past decade, many different polymerization methods have been used in the preparation of macromolecular brushes. These methods include: anionic polymerization,[36] cationic polymerization,[37] ring-opening polymerization,[12,25,38] and controlled/living radical polymerization (C/LRP).[39] Among C/LRP techniques, reversible addition−fragmentation chain transfer (RAFT) polymerization is one of the most versatile techniques due to the facile experimental setup and great potential for scale-up reactions.[40] In these years, "click chemistry" has gained a great deal of attention due to the

*Corresponding author. Telephone: 86-022-2349-8703. E-mail: hyzhao@nankai.edu.cn.

 Published on Web 08/25/2010

Scheme 1. Outline for the Synthesis of Asymmetric Macromolecular Brushes with Hydrophilic Poly(ethylene glycol) (PEO) and Amphiphilic PS-*b*-PNIPAM Block Copolymer Side Chains Based on Click Chemistry and Sequential RAFT Polymerization

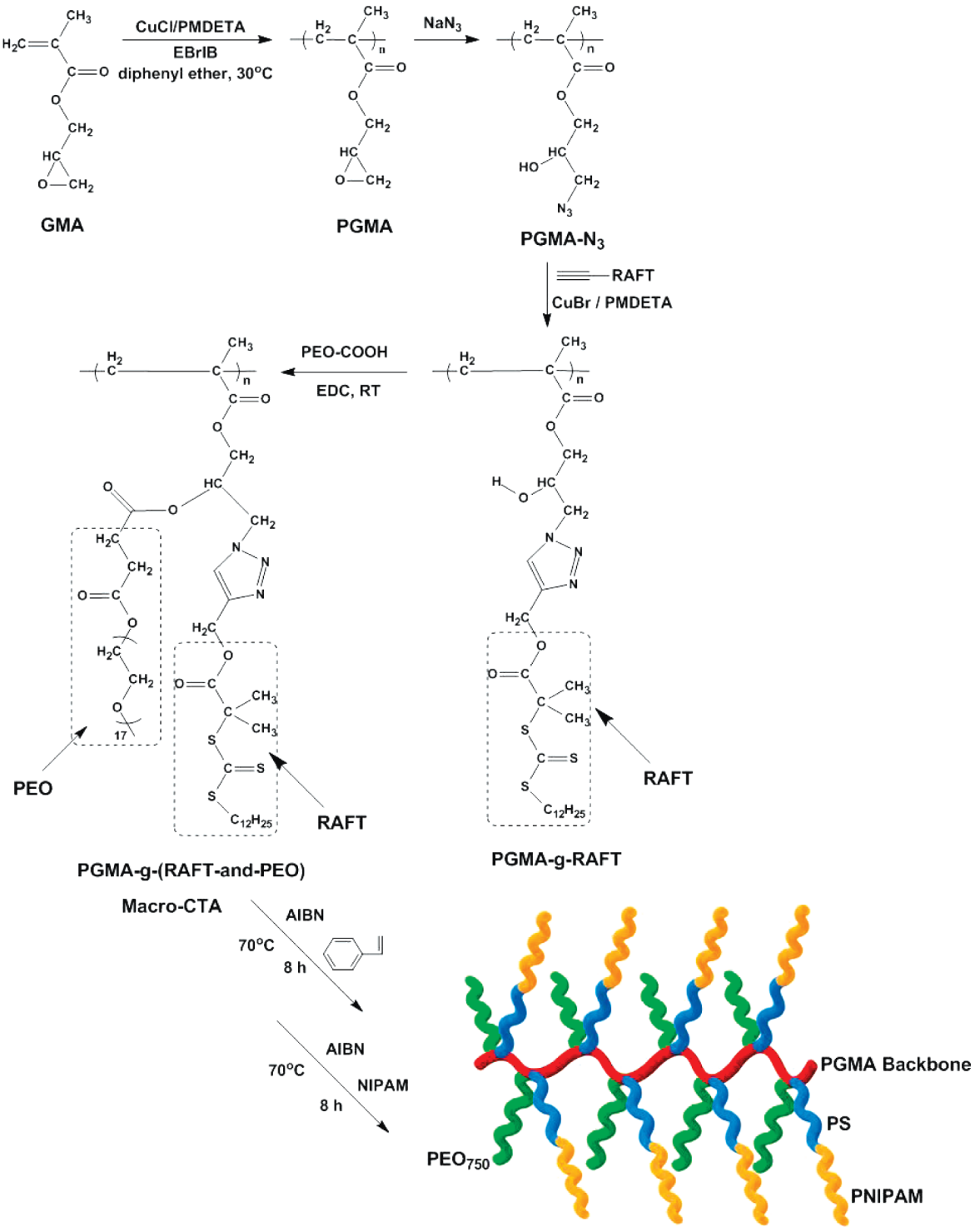

excellent functional-group tolerance, high specificity and nearly quantitative yields under mild experimental conditions.[41] The combination of C/LRP and click chemistry is an efficient way to prepare macromolecular brushes.[42] Previously, we reported synthesis of functional macromolecular brushes based on RAFT polymerization and click chemistry.[43] Herein, we report synthesis of asymmetric macromolecular brushes with hydrophilic poly(ethylene glycol) (PEO) and hydrophobic polystyrene (PS), or PEO and poly(styrene-block-*N*-isopropylacrylamide) (PS-*b*-PNIPAM) side chains based on click chemistry and RAFT polymerization (Scheme 1). Our strategy includes: (1) synthesis of polymer backbones with pendant hydroxyl groups and azide molecules by atom transfer radical polymerization (ATRP) and ring-opening reaction; (2) grafting of RAFT chain transfer agent (CTA) to polymer backbone by facile click reaction (macro-chain transfer agent); (3) covalently coupling of PEO chains to the backbone by esterification reaction; (4) synthesis of PS or PS-*b*-PNIPAM side chains by one-step or sequential RAFT polymerization. The self-assembly of the amphiphilic macromolecular brushes in solutions was also investigated in this research.

Experimental Section

Materials. CuBr (99.5%) and copper chloride (CuCl, 97%) were purchased from Guo Yao Chemical Company and TianJin Institute of Chemical Agents, respectively. Before use, they were purified by washing with glacial acetic acid, ethyl ether, and drying under vacuum. $CuCl_2$ (99%) was purchased from TianJin Ke Mi Ou Chemical Company, before use it was dried under vacuum. Disodium ethylenediamine tetraacetate (EDTA, 99%), and succinic anhydride (99%) were purchased from TianJin Chemical Company and used as received. Glycidyl methacrylate (Aldrich, 97%) was purified by distilling under reduced pressure. *N*-Isopropylacrylamide (97%) was purchased from Aldrich; before use it was recrystallized from hexane and dried under vacuum. Ethyl 2-bromoisobutyrate (EBrIB) (Aldrich, 98%), PEO with number-average molecular weight of 750 (Aldrich), 1-ethyl-3-(3-dimethyllaminopropyl) carbodiimide (EDC) (Alfa, 98%), 4-(dimethylamino) pyridine (DMAP) (Alfa, 99%), sodium azide (Alfa, 99%), tetrabutylammonium fluoride (TBAF) (Aldrich, 98%), 2-bromo-2-methyl propionyl bromide (Aldrich, 98%), *N*,*N*,*N*′,*N*″,*N*″-pentamethyldiethylenetriamine (PMDETA) (Aldrich, 99%) were used as received. *S*-1-Dodecyl-*S*′-(α,α′-dimethyl-α″-acetic acid) trithiocarbonate was synthesized according to previous literature.[44] All the solvents were distilled before use.

Preparation of Alkyne-Terminated Trithiocarbonate. Alkyne-terminated *S*-1-dodecyl-*S*′-(α,α′-dimethyl-α″-propargyl acetate) trithiocarbonate was synthesized by esterification of *S*-1-dodecyl-*S*′-(α,α′-dimethyl-α″-acetic acid) trithiocarbonate and propargyl alcohol. *S*-1-dodecyl-*S*′-(α,α′-dimethyl-α″-acetic acid) trithiocarbonate (1.03 g, 2.75 mmol), EDC·HCl (1.08 g, 5.49 mmol) and DMAP (0.035 g, 0.27 mmol) were mixed in 20 mL of dry CH_2Cl_2. Propargyl alcohol (0.30 mL, 5.2 mmol) was added dropwise to the mixture at 0 °C, and the transparent yellow solution was stirred at room temperature for 48 h. After the reaction, the mixture was washed with distilled water for three times. The ester was further purified with silica column chromatography (eluent: a mixture of petroleum ether and ethyl acetate with a volume ratio of 1:1), and *S*-1-dodecyl-*S*′-(α,α′-dimethyl-α″-propargyl acetate) trithiocarbonate was obtained. The yield of the product is about 88%.

^{1}H NMR, δ (400 MHz, $CDCl_3$, TMS, ppm): 4.69 ($-CH_2-C\equiv CH$, s, 2H); 3.25 ($-S-CH_2-CH_2-$, t, 2H); 2.46 ($-C\equiv CH$, s, 1H); 1.71 ($-CO-C(CH_3)_2-COO-$, s, 6H); 1.25−1.66 ($-C_{10}H_{20}$, m, 20H); 0.88 ($-CH_2-CH_3$, t, 3H). IR (KBr) (wavenumber, cm^{-1}): 3302 (≡C−H), 2919 and 2850 (C−H), 2132 (C≡C), 1736 (C=O), 1069 (C=S).

Synthesis of Carboxyl-Terminated PEO (PEO_{750}−COOH). A typical procedure for the synthesis of carboxyl-terminated PEO was described as follows. PEO with average molecular weight of 750 (17.0 g, 22.7 mmol), succinic anhydride (3.53 g, 35.2 mmol), DMAP (2.81 g, 22.7 mmol), and triethylamine (3.20 mL, 22.7 mmol) were dissolved in 80 mL of anhydrous 1,4-dioxane, and the reaction was carried out at room temperature for 24 h under vigorous stirring. The solvent was evaporated completely by using a rotary evaporator. The residue was dissolved in methylene chloride, and the polymer was precipitated in diethyl ether. The purified product was dried under vacuum until constant weight was reached. The yield of the product is 91%.

^{1}H NMR δ (400 MHz, $CDCl_3$, TMS, ppm): 4.26 ($-COOCH_2-$, 2H), 3.65 ($-OCH_2CH_2O-$, 76H), 3.37 (CH_3O-, 3H), 2.63 ($-OCOCH_2CH_2OCO-$, 4H).

Preparation of Poly(glycidyl methacrylate) (PGMA). PGMA was prepared by ATRP. The number-average molecular weight and the molecular weight distribution of the polymer are 4.4 K and 1.20, respectively. A typical procedure was described as follows. Degassed GMA monomer (2.0 mL, 14 mmol), PMDETA (0.084 mL, 0.41 mmol), CuCl (0.036 g, 0.36 mmol), $CuCl_2$ (0.0055 g, 0.041 mmol), and diphenyl ether (4.0 mL) were added to a dry Schlenk flask. After three freeze−pump−thaw cycles, the ATRP initiator EBrIB (0.060 mL, 0.41 mmol) was introduced into the flask by using a degassed syringe to initiate the polymerization. The polymerization was conducted in an oil bath at 30.0 °C for 70 min. The polymerization was stopped by transfer the flask into liquid nitrogen. The polymer solution was diluted with chloroform and extracted with aqueous solution of EDTA to remove the copper ions. The organic layer was concentrated by rotary evaporation, and the polymer was precipitated in hexane. After filtration, the polymer was dried under vacuum until a constant weight was reached. ^{1}H NMR, δ (400 MHz, $CDCl_3$, TMS, ppm): 4.30, 3.83 ppm ($-CO_2CH_2-$), 3.23 ppm ($-CH-CH_2-O-$), 2.84, 2.64 ppm ($-CH-CH_2-O-$). IR (KBr) (wavenumber, cm^{-1}): 1730 (C=O), 907 (epoxy group). On the basis of ^{1}H NMR result, the degree of polymerization of PGMA is 27.

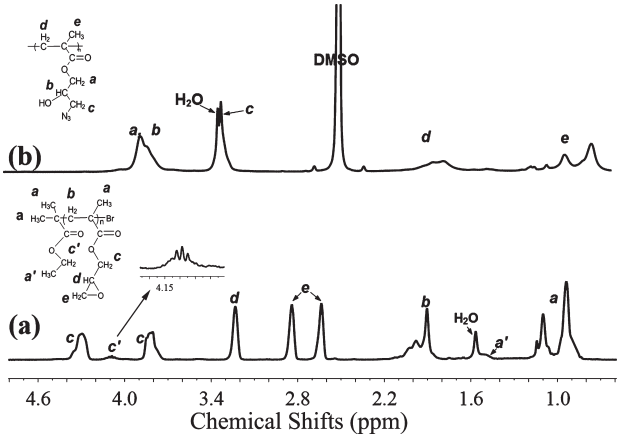

Figure 1. ^{1}H NMR spectra of (a) poly(glycidyl methacrylate) (PGMA) prepared by ATRP, and (b) its azidation product PGMA−OH/N_3, which was prepared by a reaction of PGMA and NaN_3 (3 equiv) and NH_4Cl (3 equiv) in DMF at 50 °C for 20 h. Experimental conditions of ATRP: $[GMA]_0/[EBrIB]_0/[CuCl]_0/[CuCl_2]_0/[PMDETA]_0$ = 36/1/0.9/0.1/1; $[GMA]_0$ = 3.65 M; in diphenyl ethe at 30.0 °C for 70 min. The ^{1}H NMR spectrum of PGMA was recorded in deuterated chloroform, and the spectrum of PGMA−OH/N_3 was recorded in deuterated DMSO.

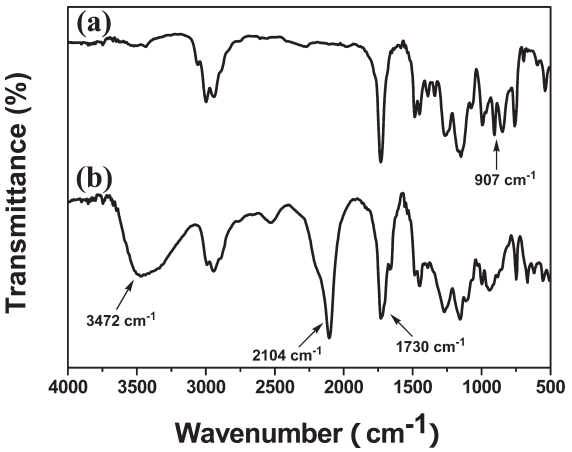

Figure 2. FTIR spectra of (a) PGMA and (b) PGMA−OH/N_3.

Ring-Opening of PGMA by Sodium Azide. PGMA (1.0 g, 7.1 mmol of epoxide groups) was dissolved in 30 mL of dry *N*,*N*-dimethylformamide (DMF). Sodium azide (1.40 g, 21.5 mmol) and ammonium chloride (1.15 g, 21.5 mmol) were added to the solution, and the mixture was stirred at 50 °C for 20 h. After removal of most DMF, poly(2-hydroxy-3-azidopropyl methacrylate) was precipitated in water, filtrated, washed with water, and dried under vacuum. In ^{1}H NMR spectrum of the polymer,

the signals representing protons on oxirane rings disappeared completely indicating the successful azidation procedure. On a polymer chain there are hydroxyl groups and pendant azide molecules; the polymer was denominated as PGMA−OH/N_3. The number-average molecular weight and the molecular weight distribution of the polymer are 3.1K and 1.05, respectively. The yield of the product is about 67%.

^{1}H NMR, δ (400 MHz, DMSO, TMS, ppm): 3.73−4.07 ppm (−COOC$\boldsymbol{H}_2$−, −COOCH$_2$C$\boldsymbol{H}$−OH). IR (KBr) (wavenumber, cm^{-1}): 3472 (OH), 2104 (C−N═N═N), 1730 (C═O).

Coupling of RAFT CTA to PGMA−OH/N_3. PGMA−OH/N_3 (0.31 g, 1.6 mmol of azide groups), alkyne-terminated RAFT CTA *S*-1-dodecyl-*S*′-(α,α′-dimethyl-α″-propargyl acetate) trithiocarbonate (1.3 g, 3.2 mmol of alkyne groups), and PMDETA (0.35 mL, 1.6 mmol) were mixed in 6.5 mL of dry DMF. The mixture was degassed by three freeze−pump−thaw cycles. CuBr (0.24 g, 1.6 mmol) was added to the solution in nitrogen atmosphere and the mixture was stirred at room temperature for 24 h. After the reaction, the solution was concentrated by rotary evaporation, and the polymer bearing CTA (PGMA−OH/CTA) was precipitated in hexane. PGMA−OH/CTA was extracted with hexane to remove unreacted RAFT CTA. The number-average molecular weight and the molecular weight distribution of the polymer are 8.4K and 1.42, respectively. The yield of the product is about 56%.

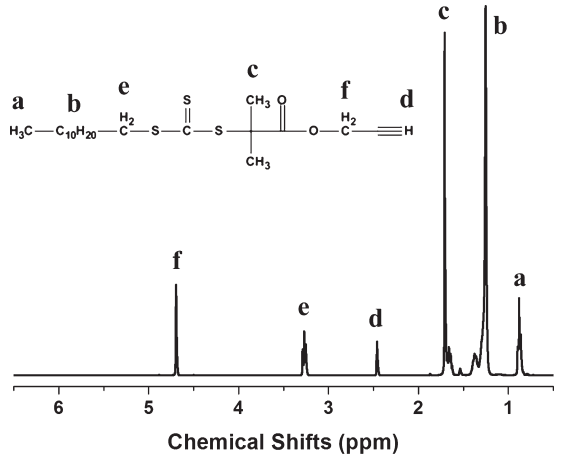

Figure 3. ^{1}H NMR spectrum of *S*-1-dodecyl-*S*′-(α,α′-dimethyl-α″-propargyl acetate) trithiocarbonate.

^{1}H NMR, δ (400 MHz, CDCl$_3$, TMS, ppm): 7.89 (triazole, 1H); 5.19 (−OCO-C$\boldsymbol{H}_2$-triazole-, 2H); 4.83−3.72 (−OCO−C$\boldsymbol{H}_2$−C$\boldsymbol{H}$(O$\boldsymbol{H}$)-C$\boldsymbol{H}_2$-triazole, 6H); 3.24 (−SCS−S−C$\boldsymbol{H}_2$−, 2H). IR (KBr) (wavenumber, cm^{-1}): 1732 (C═O), 1062 (C═S).

Coupling of PEO$_{750}$−COOH onto PGMA−OH/CTA Backbone by Esterification Reaction. The hydroxyl groups on PGMA−OH/CTA were reacted with PEO$_{750}$−COOH in the presence of EDC and DMAP in CH_2Cl_2. PGMA−OH/CTA (0.10 g, 0.18 mmol of hydroxyl groups), PEO$_{750}$−COOH (0.28 g, 0.37 mmol) and DMAP (0.0024 g, 0.018 mmol) were dissolved in 15 mL of dry CH_2Cl_2 and the mixture was cooled to 0 °C under stirring. EDC (0.074 g, 0.37 mmol) was added to the solution. After 20 min stirring at 0 °C, the solution was warmed to room temperature and stirred for 24 h. After evaporation of CH_2Cl_2, the crude product was dialyzed against water to remove the excess PEO$_{750}$−COOH and EDC. Polymer with grafted PEO and RAFT CTA (PGMA-*graft*-(PEO/CTA)) was obtained after freeze-drying. M_n = 13K, M_w/M_n = 1.37. ^{1}H NMR, δ (400 MHz, CDCl$_3$, TMS, ppm): 7.89 (triazole, 1H); 5.19 (−OCO−C$\boldsymbol{H}_2$−triazole−, 2H); 4.83−3.72 (−OCO−C$\boldsymbol{H}_2$−C$\boldsymbol{H}$(O$\boldsymbol{H}$)−C$\boldsymbol{H}_2$−triazole, 6H); 3.24 (−SCS−S−C$\boldsymbol{H}_2$−, 2H); 3.37−3.81 (−OC$\boldsymbol{H}_2$C$\boldsymbol{H}_2$OC$\boldsymbol{H}_3$); 2.65 ppm (−COOC$\boldsymbol{H}_2$C$\boldsymbol{H}_2$-COO−, 4H). IR (KBr) (wavenumber, cm^{-1}): 1731 (C═O), 1102 (C−O), 1062 (C═S).

Synthesis of PS and PS-*b*-PNIPAM Side Chains by RAFT Polymerization. Asymmetric macromolecular brushes with PS or PS-*b*-PNIPAM block copolymer side chains were prepared by one-step or sequential RAFT polymerization. PGMA-*graft*-(PEO/CTA) was used as macro-CTA in the synthesis of macromolecular brushes with PS side chains. The synthesis was described as follows. PGMA-*graft*-(PEO/CTA) (0.012 g), styrene (0.21 mL, 1.8 mmol) and AIBN (0.38 mg, 0.0023 mmol) were dissolved in 3.2 mL of dry DMF. The mixture was degassed by three freeze−pump−thaw cycles, and stirred at 70 °C for 8 h. In

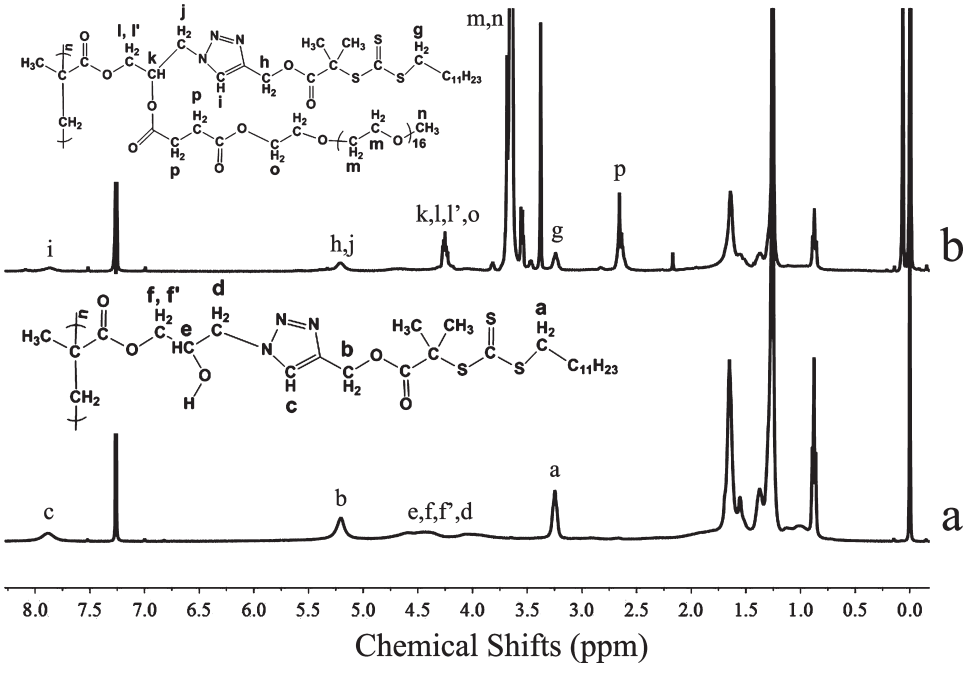

Figure 4. ^{1}H NMR spectra of (a) PGMA−OH/CTA prepared by click reaction between PGMA−OH/N_3 and *S*-1-dodecyl-*S*′-(α,α′-dimethyl-α″-propargyl acetate) trithiocarbonate (alkyne−RAFT CTA), and (b) PGMA-*graft*-PEO/CTA prepared by esterification of PGMA−OH/CTA and PEO$_{750}$−COOH. Experimental conditions of click reaction: [alkyne−RAFT CTA]$_0$/[PGMA−OH/N_3]$_0$/[CuBr]$_0$/[PMDETA]$_0$ = 2/1/1/1; [PGMA−OH/N_3]$_0$ = 0.25 M; in DMF at room temperature for 24 h.

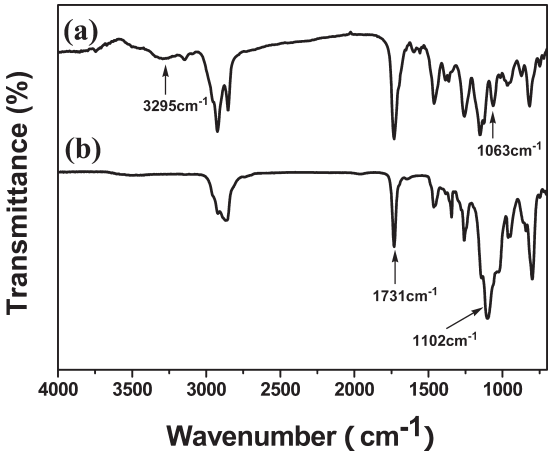

Figure 5. FTIR spectra of (a) PGMA−OH/CTA and (b) PGMA-*graft*-PEO/CTA.

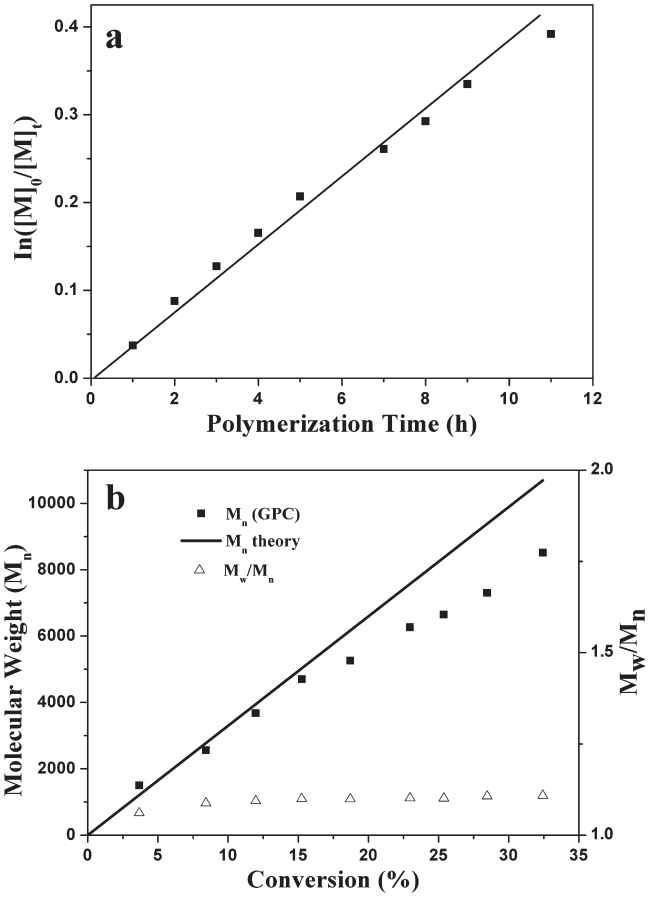

Figure 6. (a) Dependence of $\ln([M]_0/[M]_t)$ on polymerization time in the RAFT polymerization of styrene. (b) Dependence of molecular weights and molecular weight distributions on monomer conversion. In the RAFT polymerization, *S*-1-dodecyl-*S*′-(α,α′-dimethyl-α″-acetic acid) trithiocarbonate was used as RAFT CTA. Experimental conditions: $[St]_0/[CTA]_0/[AIBN]_0 = 320/1/0.25$; $[St]_0 = 8.7$ M; in DMF at 70 °C. Molecular weights of linear PS were calibrated on PS standards.

kinetic study, samples were withdrawn at different intervals for molecular weight and conversion analyses (^{1}H NMR). After the polymerization, the polymer solution was concentrated by rotating evaporation, and the polymer was precipitated in hexane. In this paper the polymer brushes with PEO and PS side chains are assigned as PGMA-*graft*-(PEO/PS$_m$), where *m* is the polymerization degree of PS side chains.

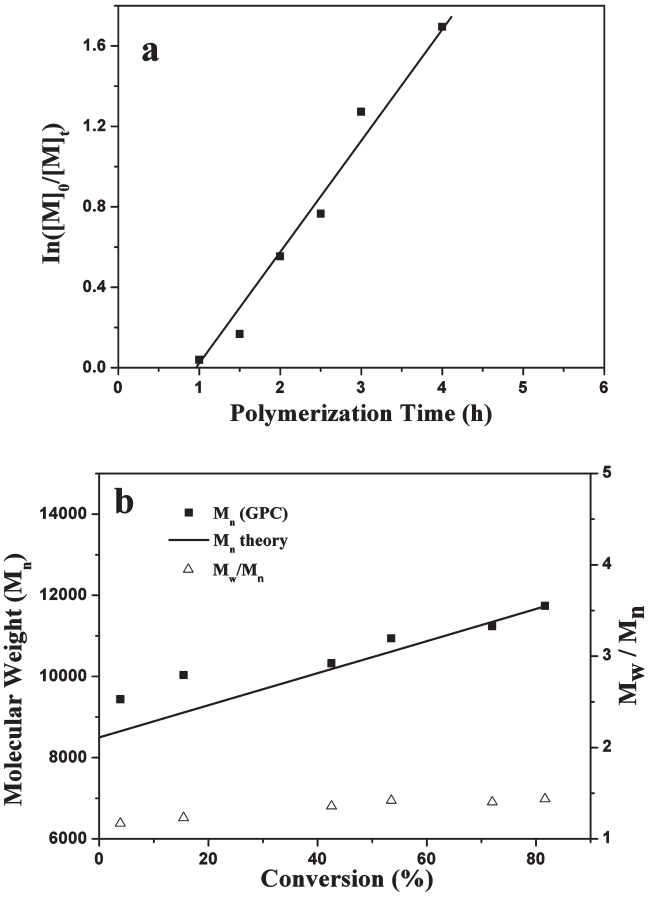

Figure 7. (a) Dependence of $\ln([M]_0/[M]_t)$ on polymerization time in the RAFT polymerization of NIPAM. (b) Dependence of molecular weights and molecular weight distributions on monomer conversion. PS macro-RAFT CTA was used in the RAFT polymerization of NIPAM. Experimental conditions: $[NIPAM]_0/[macro\text{-}CTA]_0/[AIBN]_0 = 35/1/0.25$; $[NIPAM]_0 = 0.487$ M; in DMF at 70 °C. Molecular weights of the block copolymers were calibrated on PS standards.

PGMA-*graft*-(PEO/PS) was used as macro-CTA in the synthesis of macromolecular brushes with PS-*b*-PNIPAM side chains. PGMA-*graft*-(PEO/PS) (0.006 g), NIPAM (0.055 g, 0.049 mmol), and AIBN (0.25 mg, 0.0015 mmol) were dissolved in 0.7 mL of dry DMF. The mixture was degassed by three freeze−pump−thaw cycles, and stirred at 70 °C for 8 h. After the polymerization, the polymer solution was concentrated by rotating evaporation, and the brush polymer was precipitated in hexane. In this research the asymmetric macromolecular brushes with PEO and PS-*b*-PNIPAM side chains on each repeating unit are assigned as PGMA-*graft*-(PEO/PS$_m$-*b*-PNIPAM$_n$), where *m* and *n* are the polymerization degrees of PS and PNIPAM, respectively.

Kinetic Study of Polymerization of Styrene Mediated by *S*-1-Dodecyl-*S*′-(α,α′-dimethyl-α″-acetic acid) Trithiocarbonate. In the synthesis of linear PS, *S*-1-dodecyl-*S*′-(α,α′-dimethyl-α″-acetic acid) trithiocarbonate was used as RAFT CTA. CTA (50 mg, 0.13 mmol), styrene (5.0 mL, 43 mmol) and AIBN (5 mg, 0.03 mmol) were dissolved in 5 mL of dry DMF. The mixture was degassed by three freeze−pump−thaw cycles, and stirred at 70 °C for 12 h. Samples were withdrawn at different intervals for molecular weight (GPC) and conversion analyses (^{1}H NMR). The polymerization was stopped by quenching the solution in an ice bath. The polymer was purified by precipitation in methanol.

Kinetic Study of Polymerization of NIPAM Mediated by PS Macro-RAFT CTA. Linear PS-*b*-PNIPAM block copolymer was prepared by RAFT polymerization mediated by PS

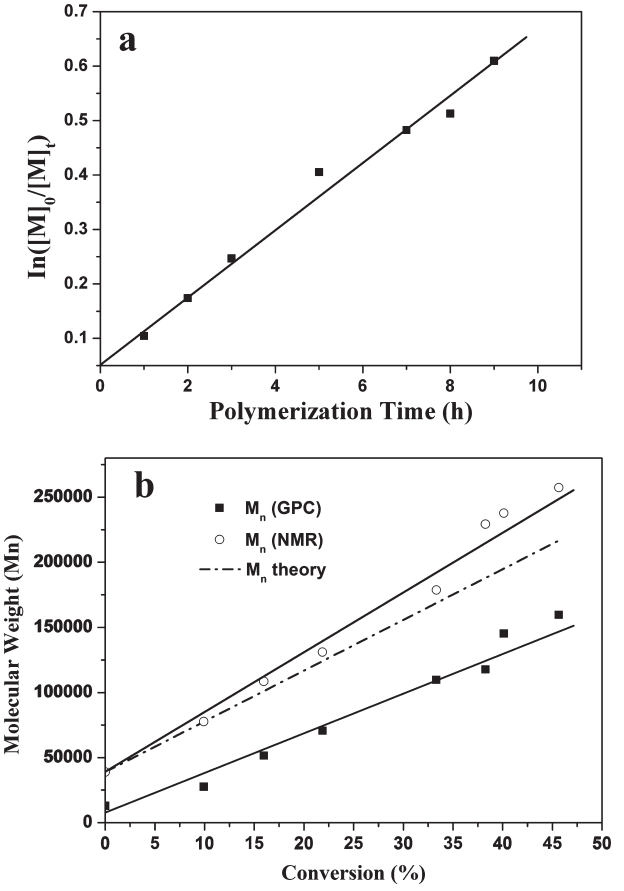

Figure 8. (a) Dependence of $\ln([M]_0/[M]_t)$ on polymerization time in the preparation of macromolecular brushes with PS side chains by RAFT polymerization. (b) Dependence of molecular weights on monomer conversion. The molecular weights were determined by GPC or ^{1}H NMR. In the RAFT polymerization PGMA-*graft*-(PEO/CTA) was used as macro-RAFT CTA. Experimental conditions: $[St]_0/[\text{macro-CTA}]_0/[AIBN]_0$ = 3600/1/0.1; $[St]_0$ = 0.87 M; in DMF at 70 °C. Molecular weights of PS brush were calibrated on PS standards.

macro-CTA. PS macro-CTA (100 mg, 0.0133 mmol), NIPAM (0.0526 g, 0.465 mmol) and AIBN (0.5 mg, 0.003 mmol) were dissolved in 1 mL of dry DMF. The mixture was degassed by three freeze−pump−thaw cycles, and stirred at 70 °C for 5 h. Samples were withdrawn at different intervals for molecular weight and conversion analyses.

Characterization. ^{1}H NMR (400 MHz) spectra of RAFT CTA and polymers were recorded on a Varian UNITY-plus 400 spectrometer using deuterated DMSO or $CDCl_3$ as the solvents. The apparent molecular weights (M_n) and molecular weight distributions (M_w/M_n) of the polymers were determined at 35 °C with a gel permeation chromatograph (GPC) equipped with a Waters 717 autosampler, Waters 1525 HPLC pump, three Waters UltraStyragel columns with 5K-600 K (10000 Å), 500−30K (1000 Å), and 100−10K (500 Å) molecular ranges, and a waters 2414 refractive index detector. THF was used as eluent at a flow rate of 1.0 mL/min. Molecular weights were calibrated on PS standards. Fourier transform infrared absorption spectra (FTIR) were obtained on a Bio-Rad FTS 6000 system using diffuse reflectance sampling accessories. UV−vis spectroscopy was performed on CaRy 100 Conc (Varian, USA) UV−visible spectrophotometer with Julabo F12 temperature control water bath. UV−vis spectroscopy (λ = 500 nm) was used for transmission measurements on samples with a concentration of 0.3 mg/mL. Transmission was monitored at temperature increment of 0.5 °C with equilibration time of 15 min. Transmission data were normalized to initial transmission at 22 °C. Transmission electron microscopy (TEM) images were obtained on a Tecnai G2

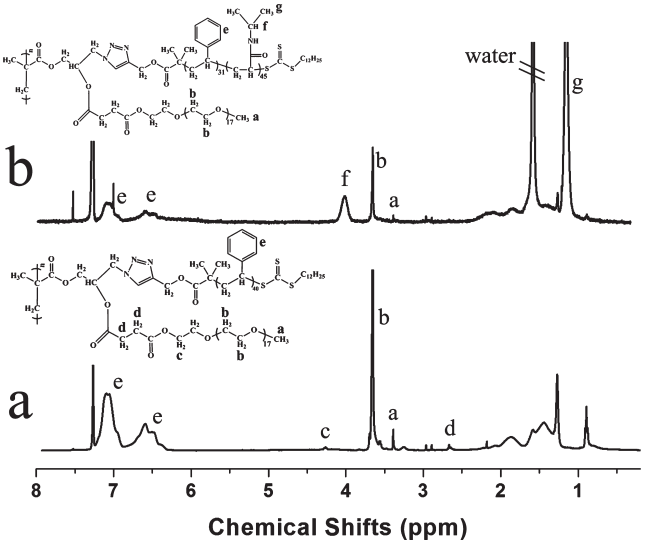

Figure 9. ^{1}H NMR spectra of amphiphilic macromolecular brushes with PS (spectrum a) and PS-*b*-PNIPAM (spectrum b) side chains prepared by RAFT polymerization. In the RAFT polymerization, PGMA-*graft*-PEO/CTA was used as macro-RAFT CTA. Experimental conditions for preparation of PS side chains: $[\text{Styrene}]_0/[\text{PGMA-}graft\text{-PEO/CTA}]_0/[AIBN]_0$ = 200/1/0.25; [styrene] = 0.58 M; in DMF at 70 °C.

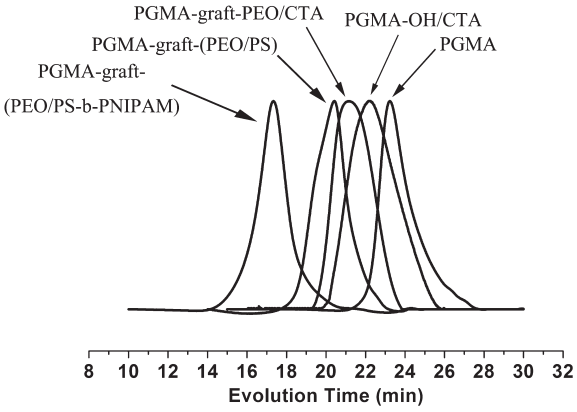

Figure 10. GPC traces of PGMA, PGMA−OH/CTA, PGMA-*graft*-PEO/CTA macro-RAFT CTA, PGMA-*graft*-(PEO/PS_{13}) and PGMA-*graft*-$(PEO/PS_{13}$-*b*-PNIPAM).

20 S-TWIN electron microscope equipped with a Model 794 CCD camera (512 × 512) at an operating voltage of 200 kV. The TEM specimens were prepared by depositing aqueous solutions of polymers on Formvar coated grids, water was evaporated in air. The TEM specimens were stained by RuO_4. The hydrodynamic diameters (D_h) of the self-assembly aggregates were measured on a Zetasizer Nano ZS from Malvern Instruments equipped with a 10 mW HeNe laser at a wavelength of 633 nm. Measurements were performed at 10 and 40 °C, and the results were analyzed in CONTIN mode.

Results and Discussion

A scheme for the synthesis of asymmetric macromolecular brushes with PEO homopolymer and PS-*b*-PNIPAM block copolymer side chains on PGMA backbone is shown in Scheme 1. PGMA homopolymer backbone was prepared by ATRP. PGMA−OH/N_3 was synthesized by opening of the oxirane rings on PGMA by sodium azide. Alkyne-terminated RAFT CTA was grafted to PGMA−OH/N_3 by click reaction. The RAFT CTA on the polymer backbone can be used in RAFT polymerization.

Table 1. Summary of Molecular Weights and Molecular Weight Distributions of Poly(glycidyl methacrylate) (PGMA), PGMA with Pendant Hydroxyl Groups and Azide Molecules (PGMA−OH/N_3), PGMA with Pendant RAFT CTA and PEO Side Chains (PGMA-*graft*-(PEO/CTA)), Macromolecular Brushes with PEO and PS Side Chains (PGMA-*graft*-(PEO/PS)), and Macromolecular Brushes with PEO and PS-*b*-PNIPAM Side Chains (PGMA-*graft*-(PEO/PS-*b*-PNIPAM))

sample	DP_{PS}[b]	DP_{PNIPAM}[b]	M_n ($\times 10^3$ g mol^{-1})[c]	PDI[c]	M ($\times 10^3$ g mol^{-1})[d]
PGMA			4.4	1.20	4.03
PGMA−OH/N_3			3.1	1.05	5.19
PGMA−OH/RAFT			8.4	1.40	16.0
PGMA-*graft*-(PEO/CTA)			13	1.37	38.9
PGMA-*graft*-(PEO/PS_{13})[a]	13		27	1.21	75.4
PGMA-*graft*-(PEO/PS_{31})[a]	31		36	1.17	125.9
PGMA-*graft*-(PEO/PS_{40})[a]	40		41	1.10	151.2
PGMA-*graft*-(PEO/PS_{31}-*b*-$PNIPAM_{53}$)[a]	31	53	56	1.10	287.7

[a] Macromolecular brushes with PEO and PS side chains, or PEO and PS-*b*-PNIPAM side chains are assigned as PGMA-*graft*-(PEO/PS_m), or PGMA-*graft*-(PEO/PS_m-*b*-$PNIPAM_n$), where *m* is the number-average degree of polymerization of PS and *n* is the number-average degree of polymerization of PNIPAM block. [b] The number-average degrees of polymerization of PS side chains and PNIPAM side chains were determined by ^{1}H NMR. [c] The number-average molecular weight (M_n) and molecular weight distribution (M_w/M_n) were measured by gel permeation chromatograph (GPC) on PS standards. [d] Molecular weights (M) were determined by ^{1}H NMR.

Macromolecular brushes with PEO side chains were obtained by an esterification reaction between PEO−COOH and hydroxyl groups on PGMA−OH/CTA. PS-*b*-PNIPAM block copolymer side chains were synthesized by sequential RAFT polymerization.

Synthesis of PGMA and (PGMA−OH/N_3). The polymerization of GMA was conducted in diphenyl ether at 30 °C with CuCl/PMDETA as catalyst and EBrIB as initiator.[45] The monomer conversion reached 75% within 70 min. The ring-opening reaction of PGMA was carried out using a method similar to the previous literature.[46] The oxirane rings were completely opened as proved by ^{1}H NMR and FTIR results. The ^{1}H NMR spectra of the starting polymer PGMA and its azidation product PGMA−OH/N_3 are shown in Figure 1. The signals of PGMA at 4.30 and 3.83 ppm represent the methene protons next to the ester groups, and the signals at 3.23, 2.84, and 2.64 ppm are attributed to the methine protons and methene protons on the rings. The signals at 3.23, 2.84, and 2.64 ppm disappeared completely after 20 h reaction, which indicated the successful ring-opening reaction by azide anion. After the reaction, new peaks at 3.73−4.07 ppm representing the methene protons next to the ester groups and the methine proton next to the hydroxyl groups (CO_2CH_2 and CH−OH), and at 3.30 and 3.32 ppm representing methene protons connected to azide groups (CH_2N_3), were observed.

In the FTIR spectrum of PGMA−OH/N_3 (spectra b in Figure 2), a strong absorbance representing the valence vibration of azide groups was observed at 2104 cm^{-1}, which confirmed the introduction of azido functionalities onto the polymer chain.[42] A broad peak at 3472 cm^{-1} attributing to the vibration of hydroxyl groups was also observed. After azidation, the absorbance band at 907 cm^{-1} corresponding to the epoxy group of PGMA[47] disappeared completely. All these results proved the high efficiency of ring-opening reaction by azide anion.

Synthesis of PGMA−OH/CTA by Click Reaction. The ^{1}H NMR spectrum and peak assignments of alkyne-terminated RAFT CTA are presented in Figure 3. Peaks at 4.69 ppm (−COO−C*H*$_2$−C≡CH) and 2.46 ppm (−C≡C*H*) can be observed, which indicates the successful reaction of *S*-1-dodecyl-*S*′-(α,α′-dimethyl-α″-acetic acid) trithiocarbonate and propargyl alcohol. Alkyne-terminated RAFT CTA *S*-1-dodecyl-*S*′-(α,α′-dimethyl-α″-propargyl acetate) trithiocarbonate was introduced onto the polymer backbone by click reaction yielding macro-RAFT CTA (PGMA−OH/CTA). The macro-RAFT CTA was used in the synthesis of block copolymer side chains by "grafting from" approach. The ^{1}H NMR spectrum of PGMA−OH/CTA is shown in Figure 4a. After the click reaction, the peak at 2.46 ppm representing the alkyne proton (−C≡*CH*) on RAFT CTA disappeared completely, and new peaks at 7.90 ppm (peak c) representing the methine proton on 1,2,3-triazole ring and at 5.20 ppm representing the two methylene protons next to the 1,2,3-triazole ring were observed, which indicated the successful 1,3-dipolar cycloaddition reaction. The peaks in the range between 3.72 and 4.83 ppm (peaks e, f, f′) correspond to the ester methylene protons and the methine proton next to the hydroxyl group. The peak at 3.24 ppm (peak a) is attributed to the methylene protons [-C(S)S−C*H*$_2$-] next to the trithiocarbonate group. The integral ratio of peak c to peak a is about 1:2, and the ratio of peak c to total area of peaks b, d, e, f, and f′ is about 1:7, which means on each GMA repeating unit there is one trithiocarbonate group.

FTIR spectrum of PGMA−OH/CTA is shown in Figure 5. In the spectrum, a strong absorbance at 2104 cm^{-1} representing the valence vibration of azide groups on PGMA−OH/N_3 (spectrum b in Figure 2) disappeared completely, and the characteristic peaks representing the trithiester groups at 1063 cm^{-1} (C═S) and the hydroxyl groups at 3295 cm^{-1} were observed.

Synthesis of PGMA-*graft*-PEO/CTA. Brush polymer bearing pendant PEO chains and RAFT CTA was prepared by reaction of PGMA−OH/CTA and PEO_{750}−COOH (Scheme 1). The ^{1}H NMR spectrum of PGMA-*graft*-PEO/CTA and the peak assignments are shown in Figure 4. After esterification, new peaks at 3.37−3.81 ppm (−OC*H*$_2$C*H*$_2$-OC*H*$_3$) (m, n) and at 2.65 ppm (−COOC*H*$_2$C*H*$_2$COO−) (p) were observed, which indicated that the PEO chains were grafted to the polymer backbone. On the basis of the ratio of the peak representing the proton on 1,2,3-triazole ring to that corresponding to the protons on PEO, the molar ratio of PEO to trithiocarbonate were obtained. Our calculation result showed that the value was 1:1, which indicated that on each GMA repeating unit there was one PEO side chain and one RAFT CTA molecule. The characteristic absorbance of PEO (ν = 1102 cm^{-1} for C−O) and trithiester group at 1063 cm^{-1} (C═S) were clearly observed in the FTIR spectrum of PGMA-*graft*-PEO/CTA (Figure 5b).

Preparation of PS and PS-*b*-PNIPAM Side Chains by RAFT Polymerization. PS homopolymer and PS-*b*-PNIPAM diblock copolymer side chains on polymer backbone were synthesized by one-step or two-step RAFT polymerization (Scheme 1). In order to investigate the living/controlled property of the RAFT polymerization of side chains, the polymerization kinetic studies on the synthesis of linear PS and PS-*b*-PNIPAM were conducted. In the kinetic studies *S*-1-dodecyl-*S*′-(α,α′-dimethyl-α″-propargyl acetate) trithiocarbonate was used as RAFT CTA in the polymerization of

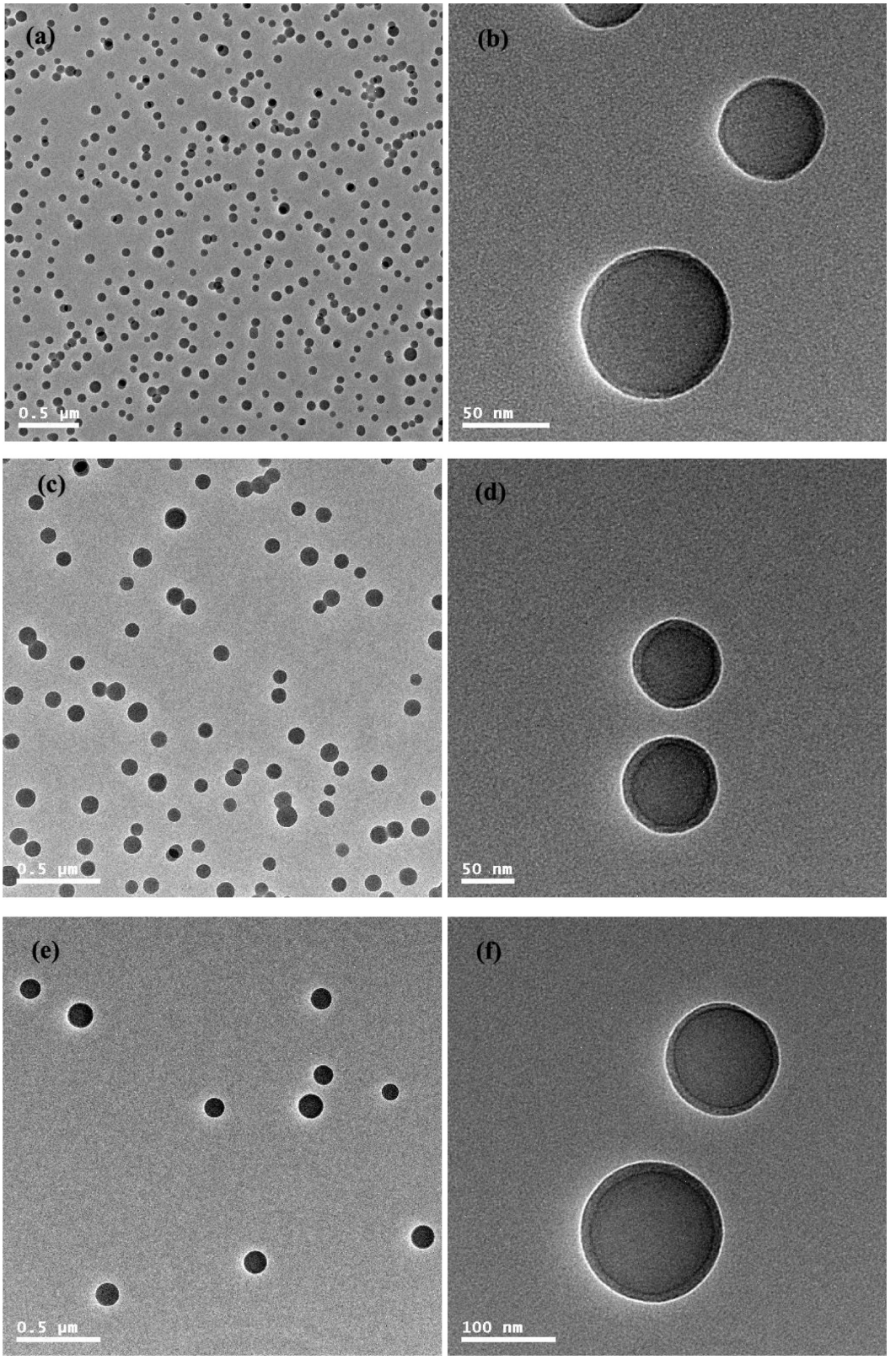

Figure 11. TEM images of self-assembly aggregates of PGMA-*graft*-(PEO/PS_{13}) (a, b), PGMA-*graft*-(PEO/PS_{31}) (c, d) and PGMA-*graft*-(PEO/PS_{40}) (e, f) in methanol.

styrene; PS macro-RAFT CTA was used in the synthesis of PS-*b*-PNIPAM. The polymerization kinetic for styrene is shown in Figure 6. A linear increase in monomer conversion with time was observed (Figure 6a), which indicated a well-controlled RAFT process by using the RAFT agent. The molecular weight of PS also increased linearly with monomer conversion, and agreed well with the theoretic values at low monomer conversion (Figure 6b). The polydispersity indices remained very low within the investigated conversion range.

The kinetics of the copolymerization of PNIPAM and PS mediated with PS macro-RAFT CTA showed similar properties of a living/controlled polymerization. After an induction

period of 1 h, the NIPAM monomer conversion increased linearly with time (Figure 7a). The molecular weight of the block copolymer increased linearly with monomer conversion, and the polydispersity indices were low (PDI < 1.25) at low monomer conversion; however, the polydispersity increased to 1.40 at high monomer conversion (Figure 7b). In order to obtain tailored diblock copolymer side chains in the preparation of macromolecular brushes, we stopped the polymerization at low monomer conversion (< 40%).

PS brushes were synthesized by RAFT polymerization by using PGMA-*graft*-(PEO/CTA) as macro-RAFT CTA and AIBN as initiator. In a kinetic study a linear relationship was observed in a plot of $\ln([M]_0/[M]_t)$ versus polymerization time (Figure 8a), indicating that the concentration of living free radicals was kept unchanged and no detectable termination occurred in the polymerization. Molecular weights of the PS brushes determined by ^{1}H NMR or GPC increased with monomer conversion (Figure 8b). It is worthy of note that the molecular weights of the brush polymers measured by GPC are lower than theoretical values or those determined by ^{1}H NMR due to the compact grafting structure of the brush polymers. Usually, intermolecular termination of living free radicals will result in cross-linking of molecular brushes. In this research, no crossing-linking was observed at low monomer conversion due to the steric hindrance of the pendant PEO side chains on backbone. It is PEO chains that prevent possible intermolecular or intramolecular free radical coupling reactions or cross-linking of the macromolecular brushes. Figure 9 shows ^{1}H NMR spectra of macromolecular brushes with PS homopolymer and PS-*b*-PNIPAM diblock copolymer side chains. On spectrum a in Figure 9, the peaks at 6.3−7.2 ppm (e) and 3.4−3.8 ppm (b) represent the phenyl protons on PS chains and methylene protons on PEO chains, respectively. Using these peaks, the molar ratio of PS to PEO can be obtained. Because the DP_n value of PEO is 17, the average DP_n of PS side chains can be calculated based on ^{1}H NMR result. Spectrum b in Figure 9 is the ^{1}H NMR spectrum of PGMA-*graft*-(PEO/PS-*b*-PNIPAM). On the spectrum, besides the signals of PS and PEO side chains, characteristic signals of PNIPAM at δ = 4.0 (f) and 1.1 (g) ppm representing methyne and methyl protons on isopropyl groups were observed, which verified the successful synthesis of diblock copolymer side chains. The average DP_n of PNIPAM blocks were obtained based on the area ratio of peak e to peak f.

The apparent number-average molecular weights and molecular weight distributions of PGMA-*graft*-(PEO/PS) and PGMA-*graft*-(PEO/PS-*b*-PNIPAM) were determined by GPC. GPC traces of an asymmetric macromolecular brush and its precursors were presented in Figure 10. It was found that the GPC trace moved to short retention time region after each step reaction or polymerization. The number-average molecular weights and molecular weight distributions of PGMA-*graft*-(PEO/PS) and PGMA-*graft*-(PEO/PS-*b*-PNIPAM), and average DP_n of PS and PS-*b*-PNIPAM side chains obtained by ^{1}H NMR were summarized in Table 1.

Self-Assembly of PGMA-*graft*-(PEO/PS) in Methanol. In PGMA-*graft*-(PEO/PS), there are one PEO and one PS side chain on each repeating unit of PGMA backbone. This structure is very similar to a macromolecular brush prepared by polymerization of diblock copolymer macromonomers at the block points. Because of the property of self-assembly of linear block copolymers in selective solvents, it is very interesting to investigate the self-assembly of PGMA-*graft*-(PEO/PS) macromolecular brushes in a selective solvent. PGMA-*graft*-(PEO/PS) with different PS chain lengths were dissolved in THF. The polymer solutions were slowly added

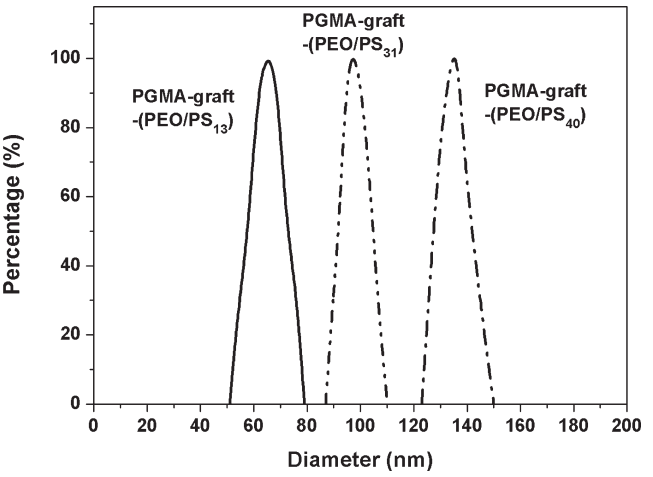

Figure 12. Size distributions of self-assembly aggregates of PGMA-*graft*-(PEO/PS_{13}), PGMA-*graft*-(PEO/PS_{31}) and PGMA-*graft*-(PEO/PS_{40}) in methanol.

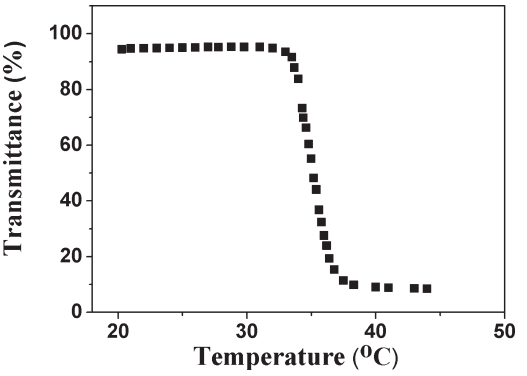

Figure 13. Transmittance changes of PGMA-*graft*-(PEO/PS_{31}-*b*-$PNIPAM_{53}$) aqueous solution with temperature.

to 6-fold of methanol, a solvent for PEO and a precipitant for PGMA backbone and PS side chains, and colloid solutions were obtained. Figure 11 shows TEM images of self-assembly aggregates of PGMA-*graft*-(PEO/PS_{13}), PGMA-*graft*-(PEO/PS_{31}) and PGMA-*graft*-(PEO/PS_{40}) in methanol. The TEM specimens were prepared by depositing polymer solutions on Formvar coated grids; methanol was evaporated in air. PS side chains were selectively stained by RuO_4. Parts a, c, and e of Figure 11 are TEM images of three macromolecular brushes at low magnification, which indicate that with the increase of PS chain length from 13 to 31 and to 40, the averages sizes of the structures increase from 67 to 97 and to 125 nm. Size analysis of the self-assembly aggregates of the macromolecular brushes based on TEM results are shown in Figure 12. It can be found that with the increase of PS chain length, the size distribution curve moves to big size region.

Parts b, d, and f of Figure 11 are TEM images of self-assembly aggregates of PGMA-*graft*-(PEO/PS_{13}), PGMA-*graft*-(PEO/PS_{31}), and PGMA-*graft*-(PEO/PS_{40}) at high magnification. On the TEM images, the appearance of the dark rings in the self-assembly structures indicates the formation of vesicular structures. PS chains in the brush macromolecules are short and they are selectively stained by RuO_4, so the thin dark rings around the structures represent collapsed PS phases. In vesicles, the collapsed PS side chains constitute the vesicle wall to avoid unfavorable interaction with methanol, while the soluble PEO chains

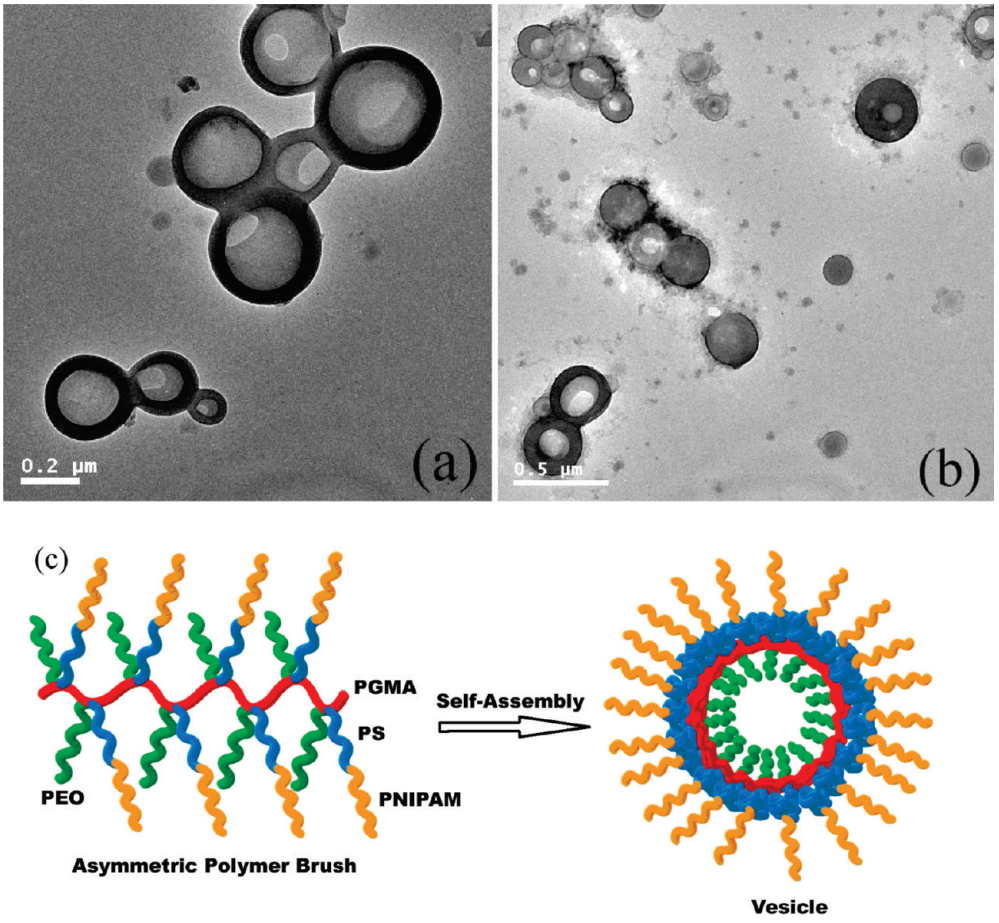

Figure 14. TEM images of self-assembly aggregates of PGMA-*graft*-(PEO/PS_{31}-*b*-$PNIPAM_{53}$) in water at 20 (a) and 40 °C (b), and a schematic representation for the self-assembly of the asymmetric macromolecular brush into vesicle structure (c).

extend from the inner and outer surfaces into methanol to stabilize the structure.

Self-Assembly of PGMA-*graft*-(PEO/PS_{31}-*b*-$PNIPAM_{53}$) Macromolecular Brush in Water. PNIPAM is a thermosensitive polymer, which undergoes phase transition at its lower critical solution temperature (LCST) because of the cooperative dehydration of PNIPAM chains and concomitant collapse of individual chains from hydrated coils to hydrophobic globules.[48−51] PNIPAM is soluble in cold water, but it becomes insoluble as the solution temperature exceeds its LCST. In this research, turbidimetry was used to measure cloud point of aqueous solution of PGMA-*graft*-(PEO/PS_{31}-*b*-$PNIPAM_{53}$) macromolecular brush. Figure 13 shows a plot of the transmittance versus temperature (a cloud point curve). The LCST value of the asymmetric macromolecular brush obtained at 50% turbidity point is about 35 °C. Xia and co-workers prepared PNIPAM with number-average molecular weight of 6.5 kDa, and the LCST of the polymer measured at 50% turbidity point was 36.3 °C.[52] Because the molecular weight of PNIPAM block in the macromolecular brush is quite similar to that of PNIPAM homopolymer used in Xia's research, the slight difference in LCST values between the two polymers is probably due to the different structures of the polymers in aqueous solutions.[53] The structure of self-assembly aggregates of PGMA-*graft*-(PEO/PS_{31}-*b*-$PNIPAM_{53}$) was investigated in this research.

To study the structure of the self-assembly aggregates of PGMA-*graft*-(PEO/PS_{31}-*b*-$PNIPAM_{53}$) asymmetric macromolecular brush in aqueous solution, TEM observation was conducted at temperatures below and above LCST of PNIPAM. The brush polymer was dissolved in THF, and 6-fold of water was added into the solution drop by drop. The solution was dialyzed against double-distilled water for 2 days to remove THF. The TEM specimens were prepared by dipping the Formvar coated grids into the aqueous solutions, water was evaporated in air. All the above operations were conducted at 20 or 40 °C. The TEM specimens were stained by RuO_4. Figure 14 shows TEM images of self-assembly of PGMA-*graft*-(PEO/PS_{31}-*b*-$PNIPAM_{53}$) in aqueous solution at 20 and 40 °C. At 20 °C, the asymmetric brush macromolecules self-assemble into vesicle structures. A vesicle structure is composed of hydrophobic wall and hydrophilic corona. Polymer chains in the corona can be directed preferentially to either the inside or the outside of the vesicles. In the present study PEO side chains and PNIPAM blocks are both hydrophilic, and both may form the corona of the vesicles. Esisenberg and co-workers ever demonstrated that the curvature of poly(styrene-*b*-acrylic acid) (PS-*b*-PAA) vesicles was stabilized by preferential segregation of long hydrophilic PAA chains toward the outside of the vesicle and short PAA chains toward the inside of the vesicle. This chain arrangement minimizes the corona chain repulsion.[54] In this research the hydrophobic PS blocks and the brush polymer backbone constitute the vesicle wall, the longer PNIPAM blocks are preferentially segregated to the outer interface and short PEO side chains to the inside interface (Figure 14c). This chain arrangement is further proved by following ^1H NMR result measured in D_2O.

At 20 °C, the soluble PNIPAM chains are stretched, PS and PNIPAM are both stained by RuO_4, and so thick dark

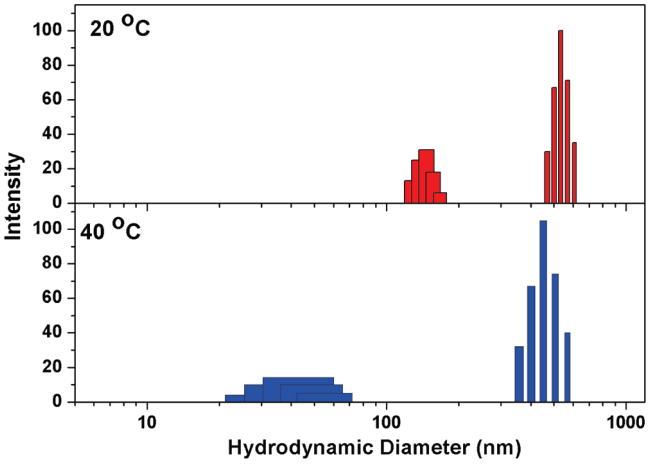

Figure 15. Size distributions of self-assembly aggregates of PGMA-*graft*-(PEO/PS_{31}-*b*-$PNIPAM_{53}$) in water at 20 and 40 °C.

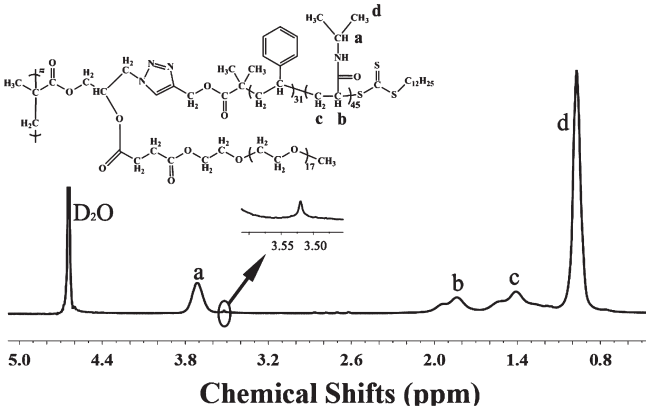

Figure 16. ^{1}H NMR spectrum of amphiphilic macromolecular brushes PGMA-*graft*-(PEO/PS_{31}-*b*-$PNIPAM_{53}$) in D_2O.

rings around the vesicle structures can be observed (Figure 14a). Vesicle structures are still maintained at 40 °C. It is worthy of note that due to the shrinking of PNIPAM blocks at this temperature, thin dark rings around vesicles can be observed (Figure 14b). The shrinking of PNIPAM in the outside corona also causes the change of vesicle size. DLS result presented in Figure 15 indicates that at 20 °C there are two populations of vesicles, one in the range from 120 to 170 nm, and the other from 465 to 615 nm. At 40 °C, there are also two broad scattering peaks on the DLS curve, one covers from 22 to 70 nm, and the other one from 348 to 567 nm. The decrease in the size of the vesicle structure is attributed to the shrinking of PNIPAM in the outside corona. At 40 °C many small dark dots with average size of 50 nm can be observed on TEM image (Figure 14b). This phenomenon can be explained by the decreased stability of the vesicles at a temperature above LCST of PNIPAM due to the transition of PNIPAM from a hydrophilic polymer to a hydrophobic polymer, and reassembly of the brush polymer into micellar structures in aqueous solution.

^{1}H NMR spectrum of PGMA-*graft*-(PEO/PS_{31}-*b*-$PNIPAM_{53}$) in D_2O is shown in Figure 16. The hydrophobic polymer backbone and PS side chains are locked in the vesicle wall, the proton signals from the hydrophobic component are suppressed; however, the proton signals of hydrophilic PNIPAM segregated to the outer interface of vesicles are prominent.[55] It is noted that on the spectrum the proton signals of PEO at 3.52 ppm are very weak. Short PEO chains are segregated to the inside interface of vesicles, the mobility of the chains are decreased due to the high curvature of the inside interface and strong repulsion of PEO chains.

Conclusions

Combination of click chemistry and RAFT polymerization is an effective strategy in the synthesis of amphiphilic asymmetric macromolecular brushes. In this research two asymmetric macromolecular brushes with different structures were synthesized. The macromolecular brushes are able to form ordered aggregates in solutions. PGMA-*graft*-(PEO/PS) brush molecules self-assemble into vesicles in methanol. The average size of the vesicles is affected by PS chain length. In aqueous solution, PGMA-*graft*-(PEO/PS-*b*-PNIPAM) brush molecules are also able to self-assemble into vesicles. Temperature exerts a significant effect on the morphology of the structures. At a temperature above LCST of PNIPAM, the size of the vesicles decreases due to the shrinking of PNIPAM in the corona.

Acknowledgment. This project was supported by National Natural Science Foundation of China (NSFC) under Contract No. 20774046.

References and Notes

(1) Hadjichristidis, N.; Pispas, S.; Floudas, G. A. *Block Copolymers: Synthetic Strategies, Physical Properties, and Applications*; Wiley-Interscience: Hoboken, NJ, 2003.
(2) Hadjichristidis, N.; Iatroua, H.; Pitsikalisa, M.; Maysb, J. *Prog. Polym. Sci.* **2006**, *31*, 1068–1132.
(3) (a) Sheiko, S.; Möller, M. *Chem. Rev.* **2001**, *101*, 4099–4123. (b) Sheiko, S.; Sumerlin, B. S.; Matyjaszewski, K. *Prog. Polym. Sci.* **2008**, *33*, 759–785.
(4) Tsukahara, Y.; Namba, S.; Iwasa, J.; Nakano, Y.; Kaeriyama, K.; Takahashi, M. *Macromolecules* **2001**, *34*, 2624–2629.
(5) Sheiko, S. S.; Prokhorova, S. A.; Beers, K. L.; Matyjaszewski, K.; Potemkin, I. I.; Khokhlov, A. R.; Möller, M. *Macromolecules* **2001**, *34*, 8354–8360.
(6) Bhattacharya, A.; Misra, B. N. *Prog. Polym. Sci.* **2004**, *29*, 767–814.
(7) Subbotin, A.; Saariaho, M.; Ikkala, O.; ten Brinke, G. *Macromolecules* **2000**, *33*, 3447–3452.
(8) Dziezok, P.; Sheiko, S. S.; Fischer, K.; Schmidt, M.; Möller, M. *Angew. Chem., Int. Ed. Engl.* **1997**, *36*, 2812–2815.
(9) Schappacher, M.; Deffieux, A. *Macromolecules* **2005**, *38*, 7209–7213.
(10) Annaka, M.; Matsuura, T.; Kasai, M.; Nakahira, T.; Hara, Y.; Okano, T. *Biomacromolecules* **2003**, *4*, 395–403.
(11) Beers, K. L.; Gaynor, S. G.; Matyjaszewski, K.; Sheiko, S. S.; Möller, M. *Macromolecules* **1998**, *31*, 9413–9415.
(12) Wu, D.; Yang, Y.; Cheng, X.; Liu, L.; Tian, J.; Zhao, H. *Macromolecules* **2006**, *39*, 7513–7519.
(13) Ishizu, K.; Tsubaki, K.; Ono, T. *Polymer* **1998**, *39*, 2935–2939.
(14) Neugebauer, D.; Zhang, Y.; Pakula, T.; Matyjaszewski, K. *Macromolecules* **2005**, *38*, 8687–8693.
(15) Neugebauer, D.; Theis, M.; Pakula, T.; Wegner, G.; Matyjaszewski, K. *Macromolecules* **2006**, *39*, 584–593.
(16) Lutz, J.; Hoth, A. *Macromolecules* **2006**, *39*, 893–896.
(17) Schappacher, M.; Deffieux, A. *Macromolecules* **2005**, *38*, 7209–7213.
(18) Baskar, G.; Chandrasekar, K.; Reddy, B. S. R. *Polymer* **2004**, *45*, 6507–6517.
(19) Ishizu, K.; Yamada, H. *Macromolecules* **2007**, *40*, 3056–3061.
(20) Ishizu, K.; Tsubaki, K.; Mori, A.; Uchida, S. *Prog. Polym. Sci.* **2003**, *28*, 27–54.
(21) Morandi, G.; Montembault, V.; Pascual, S.; Legoupy, S.; Fontaine, L. *Macromolecules* **2006**, *39*, 2732–2735.
(22) Zhang, M.; Breiner, T.; Mori, H.; Müller, A. H. E. *Polymer* **2003**, *44*, 1449–1458.
(23) Lee, H.; Jakubowski, W.; Matyjaszewski, K.; Yu, S.; Sheiko, S. S. *Macromolecules* **2006**, *39*, 4983–4989.
(24) Lanson, D.; Schappacher, M.; Deffieux, A.; Borsali, R. *Macromolecules* **2006**, *39*, 7107–7114.

(25) Wu, D.; Zhao, C.; Tian, J.; Zhao, H. *Polym. Int.* **2009**, *58*, 1335–1340.
(26) (a) Christodoulou, S.; Iatrou, H.; Lohse, D. J.; Hadjichristidis, N. *J. Polym. Sci., Part A: Polym. Chem.* **2005**, *43*, 4030–4039. (b) Koutalas, G.; Lohse, D. J.; Hadjichristidis, N. *J. Polym. Sci., Part A: Polym. Chem.* **2005**, *43*, 4040–4049.
(27) Lee, H.; Matyjaszewski, K.; Yu-Su, S.; Sheiko, S. *Macromolecules* **2008**, *41*, 6073–6080.
(28) Lanson, D.; Ariura, F.; Schappacher, M.; Borsali, R.; Deffieux, A. *Macromolecules* **2009**, *42*, 3942–3950.
(29) Stephan, T.; Muth, S.; Schmidt, M. *Macromolecules* **2002**, *35*, 9857–9860.
(30) Vasilevskaya, V. V.; Gusev, L. A.; Khokhlov, A. R.; ten Brinke, G. *Macromolecules* **2001**, *34*, 5019–5022.
(31) Gu, L.; Shen, Z.; Zhang, S.; Lu, G.; Zhang, X.; Huang, X. *Macromolecules* **2007**, *40*, 4486–4493.
(32) Li, C.; Ge, Z.; Fang, J.; Liu, S. *Macromolecules* **2009**, *42*, 2916–2924.
(33) (a) Hadjichristidis, N.; Pitsikalis, M.; Iatrou, H.; Pispas, S. *Macromol. Rapid Commun.* **2003**, *24*, 979–1013. (b) Neugebauer, D.; Zhang, Y.; Pakula, T.; Sheiko, S. S.; Matyjaszewski, K. *Macromolecules* **2003**, *36*, 6746–6755. (c) Yamada, K.; Miyazaki, M.; Ohno, K.; Fukuda, T.; Minoda, M. *Macromolecules* **1999**, *32*, 290–293.
(34) (a) Ranjan, R.; Brittain, W. J. *Macromolecules* **2007**, *40*, 6217–6223. (b) Muchtar, Z.; Schappacher, M.; Deffieux, A. *Macromolecules* **2001**, *34*, 7595–7600.
(35) (a) Fu, G. D.; Phua, S. J.; Kang, E. T.; Neoh, K. G. *Macromolecules* **2005**, *38*, 2612–2619. (b) Cheng, G.; Boker, A.; Zhang, M.; Krausch, G.; Müller, A. H. E. *Macromolecules* **2001**, *34*, 6883–6888.
(36) (a) Vazaios, A.; Lohse, D. J.; Hahjichristidis, N. *Macromolecules* **2005**, *38*, 5468–5474. (b) Koutalas, G.; Iatrou, H.; Lohse, D. J.; Hahjichristidis, N. *Macromolecules* **2005**, *38*, 4996–5001.
(37) Miyashita, K.; Kamigaito, M.; Sawamoto, M.; Higashimura, T. *Macromolecules* **1994**, *27*, 1093–1098.
(38) (a) Yuan, W.; Yuan, J.; Zhang, F.; Xie, X.; Pan, C. *Macromolecules* **2007**, *40*, 9094–9102. (b) Runge, M. B.; Dutta, S.; Bowden, N. B. *Macromolecules* **2006**, *39*, 498–508.
(39) (a) Matyjaszewski, K.; Qin, S.; Boyce, J. R.; Shirvanyants, D.; Sheiko, S. S. *Macromolecules* **2003**, *36*, 1843–1849. (b) Lord, S. J.; Sheiko, S. S.; LaRue, I.; Lee, H. I.; Matyjaszewski, K. *Macrozmolecules* **2004**, *37*, 4235–4240. (c) Sumerlin, B. S.; Neugebauer, D.; Matyjaszewski, K. *Macromolecules* **2005**, *38*, 702–708.
(40) (a) Delduc, P.; Tailhan, C.; Zard, S. Z. *J. Chem. Soc., Chem. Commun.* **1988**, *4*, 308–310. (b) Matyjaszewski, K. *Controlled/Living Radical Polymerizations Progress in ATRP, NMP and RAFT*; American Chemical Society: Washington, DC, 2000.
(41) Kolb, H. C.; Finn, M. G.; Sharpless, K. B. *Angew. Chem., Int. Ed.* **2001**, *40*, 2004–2021.
(42) O'Reilly, R. K.; Joralemon, M. J.; Hawker, C. J.; Wooley, K. L. *J. Polym. Sci., Part A: Polym. Chem.* **2006**, *44*, 5203–5217.
(43) (a) Zhang, X.; Lian, X.; Liu, L.; Zhang, J.; Zhao, H. *Macromolecules* **2008**, *41*, 7863–7869. (b) Wu, D.; Song, X.; Tang, T.; Zhao, H. *J. Polym. Sci., Part A: Polym. Chem.* **2010**, *48*, 443–453. (c) Zhao, C.; Wu, D.; Lian, X.; Zhang, Y.; Song, X.; Zhao, H. *J. Phys. Chem. B* **2010**, *114*, 6300–6308.
(44) Lai, J. T.; Filla, D.; Shea, R. *Macromolecules* **2002**, *35*, 6754–6756.
(45) Cañamero, P. F.; Fuente, J. L.; Madruga, E. L.; García, M. F. *Macromol. Chem. Phys.* **2004**, *205*, 2221–2228.
(46) Tsarevsky, N. V.; Bencherif, S. A.; Matyjaszewski, K. *Macromolecules* **2007**, *40*, 4439–4445.
(47) Espinosa, M. H.; del Toro, P. J. O.; Silva, D. Z. *Polymer* **2001**, *42*, 3393–3397.
(48) Schild, H. G. *Prog. Polym. Sci.* **1992**, *17*, 163–249.
(49) Wu, C.; Zhou, S. *Macromolecules* **1995**, *28*, 8381–8387.
(50) Yan, J.; Ji, W.; Chen, E.; Li, Z.; Liang, D. *Macromolecules* **2008**, *41*, 4908–4913.
(51) Liang, D.; Zhou, S.; Song, L.; Zaitsev, V. S.; Chu, B. *Macromolecules* **1999**, *32*, 6326–6332.
(52) Xia, Y.; Yin, X.; Burke, N.; A., D.; Stöver, H. D. H. *Macromolecules* **2005**, *38*, 5937–5943.
(53) Zhang, W.; Zhou, X.; Li, H.; Fang, Y.; Zhang, G. *Macromolecules* **2005**, *38*, 909–914.
(54) (a) Luo, L.; Eisenberg, A. *J. Am. Chem. Soc.* **2001**, *123*, 1012–1013. (b) Discher, D. E.; Eisenberg, A. *Science* **2002**, *297*, 967–973.
(55) Sun, T.; Du, J.; Yan, L.; Mao, H.; Wang, J. *Biomaterials* **2008**, *29*, 4348–4355.